

A three stage model for the inner engine of Gamma Ray Burst: Prompt emission and early afterglow

Jan Staff and Rachid Ouyed

*Department of Physics and Astronomy, University of Calgary, 2500 University Drive NW,
Calgary, AB T2N 1N4, Canada*

and

Manjari Bagchi ¹

Tata Institute of Fundamental Research, Homi Bhaba Road, Colaba, Mumbai 400005, India

ABSTRACT

We propose a new model within the “Quark-nova” scenario to interpret the recent observations of early afterglows of long Gamma-Ray Bursts (GRB) with the Swift satellite. This is a three-stage model within the context of a core-collapse supernova. Stage 1 is an accreting (proto-) neutron star leading to a possible delay between the core collapse and the GRB. Stage 2 is an accreting quark-star, generating the prompt GRB. Stage 3, which occurs only if the quark-star collapses to form a black-hole, consists of an accreting black-hole. The jet launched in this accretion process interacts with the ejecta from stage 2, and could generate the flaring activity frequently seen in X-ray afterglows. This model may be able to account for both the energies and the timescales of GRBs, in addition to the newly discovered early X-ray afterglow features.

Subject headings: gamma rays: bursts, stars: evolution, (stars:) supernovae: general

1. Introduction

With the launch of the Swift satellite (Gehrels et al. 2004), observations of early X-ray afterglows from gamma ray bursts (GRBs) have become possible (sometimes as early as 80

¹Department of Physics and Astronomy, University of Calgary, Canada AB T2N 1N4

seconds after the GRB trigger). This led to some surprising observations, most notably, the existence of one or more (sometimes giant) flares (first discussed by Burrows et al. 2005) in the early X-ray afterglow (after a few hundred seconds to several thousand seconds) whose rapid variability has been interpreted as the inner engine being active much longer than the duration of the GRB itself (see for instance Zhang et al. 2006). Figure 1 shows a canonical X-ray afterglow light curve. The early X-ray afterglow often has a very steep power-law decay, lasting up to about a thousand seconds, followed by a flattening of the light curve, which lasts for $10^4 - 10^5$ seconds. This is often overlayed with flares and bumps in the light curve. Thereafter, a “classical” decaying afterglow is seen, as it was known from the pre-Swift era. It should be noted that not every bursts exhibits all of these features. The flare(s) and the flattening of the light curve are likely due to extended inner engine activity, and, this extended inner engine activity is what we focus on in this paper.

The inner engine for the GRB in our model is an accreting quark-star formed shortly (hours) after the core collapse in a massive star. This process operates in three steps: i) the quark nova (Ouyed et al. 2002), where the core is converted to quark matter resulting in mass ejection, ii) fall back material from the supernova together with some of the matter ejected during the quark nova can form an accretion disk around the quark-star. Accretion onto the quark-star launches a jet that will overtake the shell ejected by the quark nova and is a possible location for the prompt X-ray emission. Internal shocks within the jet produce the GRB, iii) if enough matter is accreted onto the quark-star, it will collapse and form a black-hole. Continued accretion onto the black-hole can lead to an ultra-relativistic jet. Interactions between this jet and the jet from the quark-star create shocks which lead to the flaring activity frequently seen in X-ray afterglows.

In this paper we assume that the gamma-ray emission is produced by internal shocks. The afterglow is produced when the merged shell creating the gamma-ray emission interacts with the external medium in an external shock.

It should be emphasized that quark stars are hypothetical objects, that have not been observed. They have been discussed theoretically for more than thirty years (see for instance Itoh 1970). Two requirements are needed for quark stars to form. First the strange quark matter (SQM) hypothesis must hold true. This hypothesis states that SQM has a lower energy state than ^{56}Fe , thus being the ground state of hadronic matter. Quark stars are usually thought to form from neutron stars whose central density increases above a critical density. Only the more massive neutron stars are thought to be able to reach this density (Staff et al. 2006). Second, the SQM EOS must support a rather massive quark star (the mass will probably not change much in converting from a neutron star to a quark star). Optionally, a quark star can form directly in the collapse of the iron core in massive stars,

in which case the second requirement might be relaxed.

In § 2 we present our model for an inner engine for GRBs in three stages, followed by a discussion of the energies and timescales of the inner engine in § 3. Then in § 4 we discuss what happens when the jet from the black-hole and the quark-star interacts followed by a discussion of the formation of the different features in the X-ray afterglow in § 5. We devote § 6 to correlations of features seen in the early afterglow light curve, and then in § 7 we apply our model to different observed GRBs. Then in § 8 we discuss our model and finally we summarize our model in § 9.

2. The three stages of activity

In this section, we discuss the three stages in our model for the inner engine for long GRBs (see Fig. 2). These stages involve a neutron star phase, a quark star phase, and a black hole phase. The goal is to explain features (e.g. flares and flattening in early X-ray afterglow) observed in long GRBs as a result of interactions between the neutron star jet, quark star jet, and the black hole jet. In essence the interaction between these jets is more generic and could be applicable to other multi-stage models involving other engines.

2.1. Stage 1: Neutron star as the inner engine

The first stage in our model is the formation of a (proto-) neutron star from the collapse of the core in the supernova. Several suggestions on how to generate GRBs from a newly formed neutron star exist (e.g. Usov 1992; Kluzniak & Ruderman 1998; Wheeler et al. 2000; Ruderman et al. 2000; Dai et al. 2006). More elaborate models involve in addition a transition to a black hole. Here we bring in an intermediate stage where the neutron star collapses to a quark star (i.e. a quark nova) first. Our model is effectively a two-stage model since we will be mostly focusing on the interaction between the quark star ejecta and the black hole ejecta. We note however that the neutron star phase can lead to a short delay between the collapse of the iron core and the GRB, which in our model occurs during the last two stages which we describe next.

2.2. Stage 2: Quark star as the inner engine

The neutron star will accrete fall-back material from the exploding star until its density reaches deconfinement density, whereby the star is converted to a strange quark-star.

Alternatively, if the density of the compact object left behind in the core collapse is above deconfinement density, the quark-star can be formed directly in the collapse. The accreting quark-star will produce the GRB (Ouyed et al. 2005, hereafter ORV), which is discussed later.

The lifetime of the neutron star will determine whether the GRB and supernova will be seen as simultaneous (or nearly simultaneous) events, or as temporally separated events. The timescale for the conversion of the neutron star can vary dramatically, depending on the accretion rate, the spin-down rate, and how close the state of the neutron star is to a deconfined state. Observations indicate that the core collapse and the GRB are normally almost simultaneous events (Della Valle 2006), which means that stage 1 in our model is usually short or not present at all.

The quark-star will be surrounded by an accretion disk, due to fallback material from the supernova, as well as quark nova material. As the star accretes matter, it will be heated up. The decay of Goldstone bosons producing photons is the main cooling mechanism in this phase (Vogt et al. 2004). For temperatures above about 7.7 MeV these photons can escape the star, whereas for lower temperature they will be absorbed by the star (see ORV). If the star heats up above 7.7 MeV, the emitted photons will interact with accreting material and eject it. This halts accretion until the star has cooled down below 7.7 MeV again. This way, episodes of accretion and ejection will occur.

The accreting material will follow the star’s magnetic field lines towards the magnetic pole of the star. Hence, most of the ejected material will be ejected from the polar regions, and it will be collimated by the magnetic field, i.e. it is a jet (ORV). We assume an accretion rate of $\dot{m} \sim 10^{-4} M_{\odot} \text{ s}^{-1}$ onto the quark star (similar to what is expected for neutron stars, Fryer et al. 1996). Explaining the physical process that limits the accretion rate is beyond the scope of this work and is left for future work. If the accretion rate is higher, we suggest a black hole is formed quickly. This gives us a one stage model, as described in § 8.2.1.

We find that for typical values of the QS magnetic field, $B \sim 10^{15} \text{ G}$ ¹, the maximum accretion rate that can be channeled towards the polar cap² to be $\dot{m} \approx 10^{-3} M_{\odot} \text{ s}^{-1}$ (for higher accretion rates the Alfvén radius lies inside the star). For $B \sim 10^{14} \text{ G}$, the accretion rate must be smaller than $\dot{m} \approx 10^{-5} M_{\odot} \text{ s}^{-1}$ for the accretion to be channeled to the polar

¹Recent work shows that 10^{15} G magnetic fields can be obtained during QS formation due to the response of quarks to the spontaneous magnetization of the gluons (e.g. Iwazaki 2005, and references therein).

²The lack of observational evidence of a precessing jet (Beloborodov et al. 2000) is naturally explained in our model since the magnetic field immediately after birth will align with the rotational axis of the star (Ouyed et al. 2006).

cap by the magnetic field, too low for the more energetic burst but suitable for lower energy bursts and very long duration bursts.

Most photons will be emitted from the polar regions (where accretion heats up the star), and they will then interact with some of the accreting material (see Fig 3). The Lorentz factor of the ejected matter is $\Gamma = \eta_{\text{QS}} m_{\text{accr}} / m_{\text{eject}}$, with $\eta_{\text{QS}} \sim 0.1$ (Frank et al. 1992), m_{accr} and m_{eject} are the accreted and ejected mass respectively (ORV). In order to achieve Lorentz factors of the order 100, only a small fraction (10^{-3}) of the accreting material can therefore be ejected. Such a small fraction can be realized since the cooling time (and therefore the period in which photons are emitted) is of the order microseconds, whereas the heating (accretion) time is of the order milliseconds (ORV). If we assume a steady accretion, and that the photons eject an amount of mass $m_{\text{eject}} \sim \dot{m} \Delta t_{\text{em}}$ for each episode we find:

$$\frac{\Delta t_{\text{accr}}}{\Delta t_{\text{em}}} \sim \frac{m_{\text{eject}}}{m_{\text{accr}}} \sim 10^{-3}, \quad (1)$$

Δt_{accr} and Δt_{em} being the time interval for accretion and ejection during one episode respectively. However, it is likely that only a fraction of this material is ejected, leading to higher Lorentz factors. This fraction might vary from episode to episode, giving rise to varying Lorentz factors in the outflow. Internal shocks created by colliding shells in the jet accelerate electrons that emit synchrotron radiation observed as gamma rays, as in Narayan et al. (1992).

In order to produce merged shells with an internal energy of about 10^{50} erg (which is generally required to explain the energies involved in GRBs) and Lorentz factors of more than a hundred (to overcome the compactness problem; see e.g. Piran 1999), the shells must be about $10^{-6} M_{\odot}$ or 10^{27} g each. If the Lorentz factors are too large (a few thousands), internal shocks will occur too late and external shocks occur before the internal shocks can take place. This sets the upper and lower limits on the Lorentz factors required for GRBs. For $\eta_{\text{QS}} = 0.1$, this means that $m_{\text{accr}} = 10^{30} - 10^{31} \text{g} \sim 10^{-3} - 10^{-2} M_{\odot}$. A more likely scenario is that in each episode less mass is ejected, and several of these ejecta quickly merge to produce shells with mass $\sim 10^{27}$ g relaxing the constraints on m_{accr} to lower values. These shell mergers will not be observed, as they occur while the jet is still inside the exploding star. The most efficient conversion of kinetic energy to internal energy is achieved when the masses of the shells are similar, and the ratio in Lorentz factor of the colliding shells are big, at least a factor two.

The duration of the accretion process depends on the mass of the disk and the maximum temperature that the star can be heated to. ORV found that this process can last hundreds of seconds, and possibly thousands. We will assume that the accretion eventually settles into a steady state. If this accretion is not high enough to heat the star much above 7.7

MeV, the ejection will be halted or very limited and the GRB comes to an end. However, the inner engine is still actively accreting, until the disk has been depleted; this is unless the star turns into a BH before disk depletion (see next subsection for more discussion).

ORV found that 10% of the rest mass energy of the accretion disk being accreted can be used to power a jet. A quark-star can probably accrete up to $0.1M_{\odot}$ without collapsing to a black-hole. Hence $0.1M_{\odot}c^2 \approx 2 \times 10^{53}$ erg is the maximum jet energy powered by accretion onto a quark-star. We assume a radiative efficiency of 10% in shell collisions during the QS phase. This means that in our model only about 1% (or about 2×10^{51} erg) of the rest mass energy of the accretion disk surrounding the quark-star can be released as gamma rays in a GRB. Using a collimation angle of a few degrees (ORV), this corresponds to $E_{\gamma, \text{iso}} \sim 10^{54}$ erg.

The ejected shells will collide with each other as explained, and be decelerated by the interstellar medium forming an external shock. Acceleration of electrons in this shock creates the afterglow (as in the internal–external shocks model). If the outflow creating the afterglow is beamed with jet angle θ_{jet} , a jet break will be observed as $\Gamma^{-1} > \theta_{\text{jet}}$ (Rhoads 1999). This usually happens after about a day.

2.3. Stage 3: Black-hole as the inner engine

For a given temperature and equation of state (EOS), a mass-radius curve for quark-stars has a maximum, i.e. there is a maximum mass for quark-stars. As is the case for the maximum mass of neutron stars, this maximum mass depends on the EOS which is still being studied. Harko & Cheng (2002) shows that quark stars whose EOS can be approximated by a linear function of the density has a Chandrasekhar limit based on degenerate quarks. This point denotes an instability, and so if there is accretion onto a star having this maximum mass, it collapses into a black hole. We note however, that thermally induced instabilities can drive the collapse to a BH before reaching the Chandrasekhar limit (for details see Bagchi et al. 2006).

When the quark-star collapses into a black-hole, the accretion process changes dramatically. The accretion rate is of the order 0.01 to $10 M_{\odot} \text{ s}^{-1}$ in a hyperaccretion disk around black holes (Popham et al. 1999), much higher than around quark stars where surface radiation and magnetospheric effects should in principle reduce the accretion rate compared to the accretion rate onto black holes. An ultrarelativistic jet is launched from the accretion process onto the black hole as in De Villiers et al. (2005). Interaction between this jet and the slower parts of the jet from the quark-star can generate flares seen in the early X-ray

afterglow and when this jet collides with the external shock, late time bumps will be seen. Internal shocks within the black hole jet itself can also occur, which likely would lead to flares in either X-ray or gamma-ray wavelengths. Since the duration of this jet is likely short, the width of these flares would also be short. This may add to the complexity of the observed light curve.

The duration of the accretion/ejection process depends on the mass of the accretion disk after the quark-star to black-hole conversion and the accretion rate. The disk is unlikely to be more than a few solar masses, giving a maximum accretion time of about a hundred seconds. However as found by De Villiers et al. (2005), accretion onto a black-hole is a much faster process (about $1M_{\odot} \text{ s}^{-1}$), which limits the duration of the accretion process to a few seconds. This we take as a typical timescale for the accretion rate onto black-holes for the rest of this paper.

3. Inner engines timescales and energies

We can estimate the ratio between the duration of the inner engine in the black-hole stage and in the quark-star stage as:

$$\frac{t_{\text{BH}}}{t_{\text{QS}}} = \frac{\frac{m_{\text{disk,BH}}}{\dot{m}_{\text{BH}}}}{\frac{m_{\text{disk,QS}}}{\dot{m}_{\text{QS}}}} = \left(\frac{\dot{m}_{\text{QS}}}{\dot{m}_{\text{BH}}} \right) \frac{m_{\text{disk}} - m_{\text{disk,QS}}}{m_{\text{disk,QS}}} = \zeta_{\text{in}} \left(\frac{m_{\text{disk}}}{m_{\text{disk,QS}}} - 1 \right) \quad (2)$$

where $m_{\text{disk}} = m_{\text{disk,QS}} + m_{\text{disk,BH}}$ and ζ_{in} parameterizes the ratio between the accretion rate onto a quark-star and a black-hole. As typical values we use the same accretion rate onto quark stars as for neutron stars, $\dot{m}_{\text{QS}} \approx 10^{-4} M_{\odot} \text{ s}^{-1}$ (Fryer et al. 1996, in fact the accretion rate depends on the maximum temperature the star is heated to as in ORV) and $\dot{m}_{\text{BH}} \approx 1 M_{\odot} \text{ s}^{-1}$ (De Villiers et al. 2005) giving $\zeta_{\text{in}} \approx 10^{-4}$, and find that the duration of the BH era is much shorter than the QS era.

The ratio between the energy produced by the inner engine in the two stages can be found by:

$$\frac{E_{\text{BH}}}{E_{\text{QS}}} = \frac{\eta_{\text{BH}} m_{\text{disk,BH}}}{\eta_{\text{QS}} m_{\text{disk,QS}}} = \zeta_{\text{in}} \frac{m_{\text{disk}} - m_{\text{disk,QS}}}{m_{\text{disk,QS}}} = \zeta_{\text{in}} \left(\frac{m_{\text{disk}}}{m_{\text{disk,QS}}} - 1 \right). \quad (3)$$

For typical values we use $\eta_{\text{BH}} \approx 10^{-3}$ ($m_{\text{ejec}}/m_{\text{acc}} = 10^{-5}$ was found in De Villiers et al. 2005, assuming $\Gamma = 100$ this gives $\eta_{\text{BH}} = \Gamma m_{\text{ejec}}/m_{\text{acc}} = 10^{-3}$), and $\eta_{\text{QS}} = 10^{-1}$ (similar to the efficiency in neutron stars, Frank et al. 1992). This gives $\zeta_{\text{in}} = 10^{-2}$. Hence, most of the energy will be output during the QS era, unless almost all of the disk ($> 99\%$) is accreted during the black-hole era.

We can now combine the two above expressions, to get a simple ratio:

$$\frac{t_{\text{BH}}}{t_{\text{QS}}} = \frac{\zeta_{\text{m}}}{\zeta_{\text{m}}} \frac{E_{\text{BH}}}{E_{\text{QS}}}. \quad (4)$$

From Eq. 3 we find that if 10% of a disk is accreted onto a quark-star (which then collapses into a black-hole) and the rest is accreted into the black-hole, the energy output in a jet from the quark-star is ten times larger than the energy output in a jet from the black-hole. In this case we see from Eq. 4 that the duration of the accretion process onto the quark-star is a thousand times longer than the duration of the accretion into the black-hole.

The above discussion is valid for the inner engine. We will now try to relate that to observations. We assume a direct relation between the energy output from the inner engine in the black-hole and quark-star phases and the observed energies from the two phases:

$$\begin{aligned} E_{\text{BH,obs}} &\simeq \langle \zeta_{\text{sh,BH}} \rangle E_{\text{BH}} \\ E_{\text{QS,obs}} &\simeq \langle \zeta_{\text{sh,QS}} \rangle E_{\text{QS}}, \end{aligned} \quad (5)$$

where $\langle \zeta_{\text{sh,BH}} \rangle$ and $\langle \zeta_{\text{sh,QS}} \rangle$ is the energy conversion efficiency in the shocks averaged over the entire duration of the shock activity (e.g. Kobayashi et al. 1997). For multiple shocks, we assume this efficiency to be the same for the jet from the black-hole and the quark-star, hence $\langle \zeta_{\text{BH}} \rangle \simeq \langle \zeta_{\text{QS}} \rangle$. Using this, we obtain the following ratios between the observed energies and the accreted masses:

$$\frac{E_{\text{BH,obs}}}{E_{\text{QS,obs}}} \simeq \frac{E_{\text{BH}}}{E_{\text{QS}}} \simeq \zeta_{\text{m}} \left(\frac{m_{\text{disk}}}{m_{\text{disk,QS}}} - 1 \right) \quad (6)$$

To a first approximation we can assume that $E_{\text{QS,obs}}$ is the observed GRB energy, and $E_{\text{BH,obs}}$ is the observed energy in flares and bumps in the X-ray afterglow.

The observed energies in X-ray flares and bumps compared to the observed energies released in gamma rays varies a lot in different bursts (from no flares or bumps to flares with fluence equal to the GRB fluence). If we take

$$\frac{E_{\text{BH,obs}}}{E_{\text{QS,obs}}} \simeq 10^{-2} \quad (7)$$

then, in our model, it would imply that

$$m_{\text{disk,BH}} \simeq m_{\text{disk,QS}}. \quad (8)$$

In other words, an equal amount of mass is accreted onto the quark-star and the black-hole. This holds true if we neglect the energy carried by the slow shells from the quark-star, causing

the flattening of the early X-ray afterglow light curve. This is a reasonable assumption, since the energy in the flattening is less than in the GRB itself.

As for a direct comparison of the time scale of the inner engine to the observed time scale, this is not possible since this is rather dictated by the complex interaction between the black hole ejecta and the quark star ejecta as we show next.

4. Interaction between black-hole ejecta and quark-star ejecta

Figure 4 illustrates the process of flattening the X-ray light curve and generating X-ray flares and bumps. If the quark-star emits low-Lorentz factor shells at late stages of shell emission, the shell from the black-hole can catch up with the last shell and produce an X-ray flare via internal shocks. This merged shell may be capable of colliding with other slow shells from the quark-star, whereby more X-ray flares will be seen, an idea bearing resemblance to what is discussed in Zou et al. (2006). The energy output from the collisions depends on the difference in Lorentz factor of the colliding shells. This is likely highest in the first collision. However, the energy also depends on the masses of the colliding shells, so the energy output is not necessarily highest in the first X-ray flare (see eqs. A3 and A4).

If the mass and Lorentz factor of the merged shell producing the X-ray flare(s) are high enough, a bump can be seen in the X-ray afterglow light curve as this shell collides with the external shock from the GRB.

The pulse width of the X-ray flares are generally longer than the width of the flares in the GRB. There are also indications that later occurring flares are wider than flares occurring early (Zhang et al. 2006). Qualitatively this can be understood from Eq. A1 in the Appendix. The width of the burst is proportional to the separation of the colliding shells. The shells creating the GRB were all produced by the quark-star in a fairly short time, whereas the black-hole shell was created long thereafter.

Our model seems capable of explaining why later flares have a longer duration. From Eq. A1 it is seen that the duration (for equal mass shells) depends on the initial distance between two shells. Since the flares in our model are all due to the jet from the black-hole colliding with slower parts of the quark-star jet, later flares are created by shells that were farther away from the black-hole jet initially. This leads to longer duration.

The flattening of the X-ray light curve is due to lower Lorentz-factor shells emitted in the later stages of the quark-star jet. These shells will catch up with the external shock from the GRB at later stages, slowly re-energizing the external shock. This is reminiscent

of the refreshed shocks scenario in Sari & Mészáros (2000). Hence the re-energization is independent of the black-hole. The flare does depend on the black-hole formation, and also on the fact that the quark-star jet emitted slower shells. A flare does not necessarily lead to flattening, as only one slow shell from the quark-star is needed to produce a flare, whereas a more continuous sequence of low-Lorentz factor shells is needed to produce the flattening.

The external shock will be decelerated by the surrounding medium. A low Lorentz factor shell will catch up with the external shock when this has decelerated to a comparable Lorentz factor. The range in Lorentz factors of the slow part of the quark-star jet is necessary to explain a given flattening therefore depends on the deceleration of the external shock, which is not well known. Following Falcone et al. (2006), a slow shell with Lorentz factor of about 20 will catch up with the external shock after $t = 10^4$ seconds, assuming a uniform external medium with density $n = 10 \text{ cm}^{-3}$. A shell with a Lorentz factor $\Gamma \sim 9$ will catch up with the external shock after $t = 10^5$ seconds.

5. Light curve features: *timescales and energies*

In this section we first summarize the light curve features that our model can produce (see Fig. 4), and then we discuss the different possible lightcurves (Fig. 5).

Steep decay: The steep decay commonly seen in the early afterglow ($t \approx 10^2 - 10^3$ seconds) is due to the curvature effect (Kumar & Panaitescu 2000). This is prompt gamma radiation from parts of the jet directed at an angle relative to the line of sight. Because of the large Lorentz factors involved, most of the radiation is beamed with a beaming angle Γ^{-1} . Some of it will be directed to angles outside of Γ^{-1} , but then softened by a Doppler factor. This is why what is seen as gamma rays along the line of sight is seen as X-rays at an angle from the line of sight. The steep decay continues until the luminosity from the external shock is dominant. This effect is dominant only because the central engine does not produce any visible activity, and the external shock is too weak to be seen.

Flattening: The flattening of the light curve is due to the external shock being re-energized by low Lorentz factor shells emitted from the quark-star. These shells catch up with the decelerating external shock. These shells were among the last ejected from the quark star. It is important to note that there is not a one-to-one ratio for the duration of the inner engine and the observed radiation in this case. The inner-engine ejection of shells could last for some hundred seconds, whereas the re-energization can last for $10^4 - 10^5$ seconds.

Flares: The flares are caused by interaction between a jet launched by a black-hole and the slower parts of the ejecta from the quark-star. In order for flares to occur, the quark-star

must have accreted enough matter that it collapses to a black-hole. The shell ejected by the black hole can be very massive, $m_{\text{BH}} \sim 10^{28}$ g and have a very large Lorentz factor. The shells ejected in the quark-star phase are likely less massive, however some of these might merge into massive ones before the black-hole shell interacts with them. In this case more than 10^{51} erg can be converted in one flare. The pulse width depends on the initial separation of the shells and on the width of the rapid shell (Kobayashi et al. 1997). The black hole shell can be fairly wide initially, and it is not unlikely that it spreads more before it collides with the quark-star shell. Finally, we mention recent work by (Liang et al. 2006) where a zero time point (right before the beginning of the flare) was taken as a signature of the reactivation of the engine. If true, this observation suggests that the engine reactivates more than once which cannot be reconciled with our model. We will tackle this issue elsewhere.

Bump: The bumps seen at late times ($t \sim 10^4 - 10^5$ seconds as in GRB 050502B; Falcone et al. 2006) are the result of the black-hole jet or the merged jet colliding with the external shock. The black-hole jet may or may not have interacted with shells from the quark-star to create flares before colliding with the external shock.

If there are no, or only a few, slow shells from the quark-star that the black-hole jet collides with, the black-hole jet might not be slowed down significantly and it will catch up with the external shock at an earlier stage. If this happens, a flare with not too steep rise will result. However, after this flare, there will be no flattening, and no bumps. The black-hole jet’s collision with the external shock marks the end of the inner engine’s contribution to the observed afterglow light curve. Thereafter, a “classical” afterglow decay is the result, with a possible jet break due to non-isotropic ejecta creating the afterglow.

There is a correlation between the energy emitted in the flares and in the bump (see § 6), so that bursts with more significant flares will have less pronounced bumps, and vice versa. This is assuming that a black-hole was formed and an equal sized disk formed around the black-hole. A small disk around the black-hole will lead to weak or no flaring and bumps. In the case when no black-hole formed, no flares and no bump will be seen.

5.1. Generic light curves in our model

Here we discuss the eight different types of light curves that our model can generate (Fig. 5).

Case 1. This case has all the properties discussed in the previous section *i.e.* flares, flattening and a late time bump. The flares are produced when a black-hole jet collides with slower shells from the quark-star. The flattening is due to slower shells from the quark-star

re-energizing the external shock, whereas the bump occurs when the black-hole jet collides with the external shock. This case is also shown in Fig. 4.

Case 2. This case shows a light curve with one or more flares and a flattening of the X-ray afterglow light curve, but no bump. This will happen if the later stages of the ejection from the quark-star produces slower shells. These slower shells will re-energize the external shock, whereby the light curve is flattened. The accretion onto the black-hole launches an ultrarelativistic shell, and when this interacts with a slower shell from the quark-star, an X-ray flare is seen. However, the merged shell from the black-hole and the quark-star jet is not fast enough to catch up with the external shock, so no bump is seen.

Case 3. This case shows flattening and a bump, but no flares. This is because the shell from the black-hole did not interact with any of the slower shells from the quark-star. This indicates that the black-hole shell was fairly slow. When the black-hole shell collides with the external shock, a bump is seen. As before, slower shells in the quark-star jet re-energizes the external shock, which flattens the light curve.

Case 4. This case has a bump, but no flare and no flattening. This occurs when the quark-star jet does not produce any late time shells that can flatten the light curve, and the shell from the black-hole can not interact with any shells to create a flare. A bump is seen when the shell from the black-hole jet collides with the external shock.

Case 5. This case has a flare and a bump, but no flattening. This is rather similar to case 4, however the quark-star jet emitted one or a few low Lorentz factor shells that the black-hole jet interacted with. This happened before the late shells from the quark-star collided with the external shock, so no flattening was created. GRB 050502B is an example of a burst in this category.

Case 6. This case shows flattening, but no flare and no bump. This occurs when the quark-star emits low Lorentz factor shells that can flatten the light curve, but no black-hole was formed, or the jet from the black hole was too weak to make any observable signatures.

Case 7. This case is similar to case 6, but the quark-star did not emit late time shells, so no flattening is seen.

Case 8. This case shows flaring, but no flattening and no bump. This occurs when the quark-star generates some slow shells and a black-hole is formed. The jet from the black-hole interacts with the slow shells and produces flaring. However, in this process the jet is slowed down enough that it cannot make any significant impact on the external shock.

Case 1a. In many observed afterglows the X-ray afterglow decays very steeply just after the end of the gamma ray emission. We have explained this as being due to the

curvature effect, that is an off-axis gamma ray emission, that in other directions is seen as the prompt emission. However, in some bursts this steep decay is not observed. Instead the X-ray afterglow declines gradually, with a power law similar to the decline at late times ($t > 10^5$ seconds). We suggest that in this case the external shock sets in earlier. There is still the possibility of having flares and flattening in the same way as before, when the jet from the black-hole collides with slower shells from the quark-star or the slower quark-star shells re-energize the external shock.

6. Light curve features: *Correlations*

6.1. Anti-correlation between X-ray flares and bumps

We have proposed that the jet launched by the black-hole is responsible for the X-ray flares and bumps. The flares are produced when the black hole jet collides with slower parts of the jet from the quark-star. The bumps seen at later times in the X-ray afterglow are due to the black-hole jet colliding with the external shock.

In Fig. 6 we explore the amount of energy converted and the resulting Lorentz factor of the merged shell when the black-hole jet with Lorentz factor $\Gamma = 100$ and mass $m = 3 \times 10^{28}$ g collides successively with N quark-star shells. We show four different cases, when the quark-star shells have Lorentz factors $\Gamma = 10, 20, 30$, or 40 and mass $m = 3 \times 10^{27}$ g (see Eqs A3 and A4 in the Appendix). In the first couple of collisions, the difference in Lorentz factor is fairly large, so a lot of energy is converted. However, after about 15 to 20 collisions, not much more energy is converted. This is because the Lorentz factors of the colliding shells are not very different. Several consecutive collisions will lead to several flares. We also see that if the Lorentz factor of the slow shells are high, the merged shell will get a higher Lorentz factor but less energy will be converted.

The energy released in the bump depends on the kinetic energy of the black-hole jet (or the merged jet that produced the flares) when it collides with the external shock. If the jet is not very energetic, i.e. a lot of energy was lost due to flaring, a weak bump will be seen. If not much energy was lost due to flaring, because there were no slower shells from the quark-star, the bump can be more pronounced.

To summarize: *Since both the flares and the bump are generated by the black-hole jet, the maximum energy available to do so is the initial kinetic energy of the jet. If a large fraction of this energy is used to produce flares, less is available for the bump, and vice versa.* This is in agreement with O’Brien et al. (2006a,b), who find that there is a correlation between the energy output in flares and in what they call the hump in observed GRB afterglows. The

hump is the flattening starting from about $t = 10^3$ seconds and includes possible bumps.

6.2. Correlation between prompt gamma energy and early X-ray afterglow energy

The total energy output from the quark-star inner engine is $\eta_{\text{QS}} m_{\text{disk,QS}} c^2 \approx 2 \times 10^{52} \text{erg}$ for $m_{\text{disk,QS}} \sim 0.1 M_{\odot}$. This energy is shared between the prompt GRB³, the external shock creating the decaying afterglow, and the re-energization of the external shock creating the flattening of the early X-ray afterglow light curve. A GRB with low energy in a prompt gamma-ray phase has more energy available for the early X-ray afterglow. Note however, that in the early X-ray afterglow more energy can be emitted by the black hole jet interacting with the quark star ejecta, as explained in the previous section.

7. Case study

In this section we will apply our model to a few observed X-ray afterglows that illustrate the different properties of our model: flares, flattening and bumps.

7.1. GRB 050219A (case 2)

The observed light curve with the X-ray telescope (XRT) and the Burst Alert telescope (BAT) do not look like they agree in this burst. This apparent discontinuity was first reported in Tagliaferri et al. (2005) and may be due to an early X-ray flare (as proposed by O’Brien et al. 2006a) after about 90 seconds. Since this flare is so early, it may either be a late internal shock produced purely by the quark-star, or possibly the result of an early black-hole formation. The early steep decay after this proposed flare is either the end of the flare or more likely due to the curvature effect (Mészáros 2006). At later stages (from about 800 seconds) the light curve flattens and there are some small flares. These are the late and slow parts of the quark-star jet that re-energize the external shock. If we are right in our assumption that there is an early flare after about 90 seconds, this would correspond to case 2 in Fig. 5.

³ For a 10% radiative efficiency during shell collisions (as in the internal-external shocks model) in the quark-star phase this would imply that a maximum of about $2 \times 10^{51} \text{erg}$ is released as synchrotron radiation.

7.2. GRB 050502B (case 5)

GRB 050502B shows a very strong X-ray flare, starting after about 350 seconds and peaking around 700 seconds (Falcone et al. 2006). In addition, there is one (or possibly two) bumps seen at about 40000 to 50000 seconds after the GRB trigger. The observed fluence of the flare is comparable or even bigger than the GRB fluence. There are indications of substructures within the flare itself. The total energy of the flare (or the GRB) is not known. We find by using Eqs. A3 and A4 that a black-hole jet of $m_r = 3 \times 10^{28}$ g, moving with Lorentz factor of $\Gamma_r = 200$ and colliding with a shell from the quark-star with Lorentz factor $\Gamma_s = 10$ and mass $m_s = 5 \times 10^{27}$ gives an internal energy $E_{\text{int}} = 2.4 \times 10^{51}$ ergs and a Lorentz factor of the merged shell of $\Gamma_m = 96$. The mass of the slow shell from the quark-star may seem large, but this can be the result of collisions at earlier times. These collisions may not have left observable flares if the difference in Lorentz factors in the colliding shells were not large or these collisions could have been part of the GRB itself. The black-hole must have ejected a fairly large amount of mass (3×10^{28} g), indicating that the accretion disk must have been fairly large.

The bump(s) at $t > 10^4$ seconds occur when the merged shell that created the flare catches up with the external shock (as suggested in Falcone et al. 2006). The underlying decay of the afterglow is due to the external shock. This burst corresponds to case 5 in Fig. 5.

7.3. GRB 050421 (case 1, 2, 5 or 8)

GRB 050421 shows two flares in the early X-ray afterglow, the first flare peaking after 111 seconds and the second after 154 seconds (Godet et al. 2006). The duration of the gamma ray emission was about 10 seconds. We remind the reader that these flares are due to a jet from a black-hole colliding with slower parts of the jet from the quark-star. The width of the first peak is about 10 seconds. This can be achieved if the quark-star emits a slow shell about 90 seconds following the first shell (c.f. eq. A1):

$$\delta t = \frac{L}{ac} = \frac{c\Delta t}{ac} = \frac{20}{2} = 10 \text{ s} \quad (9)$$

(Δt being the time interval between the emission of the quark-star shell and the black-hole shell). Alternatively, if the slower shell is emitted at the end of this burst (after about 10 seconds) but the jet from the black-hole has a significantly higher Lorentz factor, about 10 times higher than the quark-star shell :

$$\delta t = \frac{L}{ac} = \frac{100c}{10c} = 10 \text{ s}. \quad (10)$$

The second flare is created when the merged shell creating the first flare collides with another slow shell emitted from the quark-star. The later stages of this afterglow ($> 10^3$ seconds) are not observed. Therefore we cannot say if there is any flattening or bump. This corresponds to any one of cases 1, 2, 5 or 8 in Fig. 5.

Alternatively, these two flares could both be produced by internal shocks from shells created in the late stages of the accretion onto the quark star.

7.4. GRB050401 (case 6 without steep decay)

An example of a GRB without the early steep decline is GRB050401 (De Pasquale et al. 2006). The afterglows declines gradually with a decay index $\alpha \approx 0.65$ (Panaitescu et al. 2006) until about 4300 seconds. After this, the decay is steeper with a decay slope $\alpha \approx 1.39$. We ascribe the behavior until about 4300 seconds as flattening due to slower quark star shells re-energizing the external shock. There is no clear evidence of any flaring in this afterglow, in which case no black-hole jet interacted with the quark star jet or the external shock. This corresponds to case 6 without the initial steep decay.

The isotropic equivalent energy of this burst is about $E_{\gamma,iso} \sim 3 \times 10^{53}$ erg. Assuming a beaming angle of 5° , this gives a total energy in gamma rays of about 4×10^{50} erg (for a bipolar jet). Zhang et al. (2006) found that almost five times as much energy was injected in this burst during the afterglow than during the prompt gamma radiation, meaning about 2×10^{51} ergs was released in the early X-ray afterglow. In our model, this corresponds to $0.1M_\odot$ disk being accreted onto a quark star with 10% of the accreted energy ejected into a bipolar jet, and only about 2% of the jet energy goes into radiation. Most of the jet energy (the remaining 98%) is used to re-energize the external shock.

8. Discussion

8.1. Hypernova-GRB association in our model

The formation of the quark-star through a quark nova (between stage1 and 2) shortly after the core collapse or directly in the core collapse releases an extra amount of energy that can re-energize the SN ejecta, reminiscent of a hypernova (Ouyed et al. 2002; Keränen et al. 2005). GRBs seem to be associated with hypernovae (i.e. GRB 030329; Hjorth et al. 2003), (GRB 980425; Galama et al. 1998), however, the opposite is not always true (i.e. SN 2002ap; Mazzali et al. 2002, although a lack of GRB observation does not necessarily mean that no

GRB occurred). In order to get a hypernova, the energy from the conversion to quark matter is necessary. In our model, the GRB is produced by the jet launched by accretion onto the quark star. If a black hole is formed directly in the collapse (no quark star stage), there will be no hypernova. Accretion onto the black-hole can launch a jet, and internal shocks in the jet can produce a GRB (see § 8.2.1). However, since there is only one stage, there can be no late activity.

8.2. SN-less GRBs in our model

GRB060614 and GRB060505 were apparent nearby, long duration GRBs that showed no sign of a supernova, leading to the term SN-less GRBs (Fynbo et al. 2006). In the literature possible explanation for this have been that not enough ^{56}Ni is formed in the explosion (Tominaga et al. 2007), or that this is a very long and energetic “short” burst (Zhang et al. 2007). Here we give a possible interpretation of this phenomena within our model. We suggested above that the energy released by the quark nova (formation of a quark-star) could potentially lead to a hypernova. However, if the star is too massive to explode even with the extra energy released from the quark nova it will instead collapse and no supernova/hypernova will be seen. We assume that a hyperaccretion disk can form around the quark star while most of the star is trying to explode⁴, and as before accretion onto the quark-star powers an ultrarelativistic jet giving rise to a GRB. In this scenario a black-hole is the most likely final outcome: either the envelope falls back directly onto the compact core, or it feeds to the accretion disk. In the first case a black hole is formed but no ultrarelativistic jet is launched from the accretion onto it and hence no flaring or bump activity is seen in the early X-ray afterglow. In the second case the quark-star collapses to a black hole when it has accreted enough mass and continued accretion onto the black hole will launch an ultrarelativistic jet that can give rise to flaring and bump activity seen in the early X-ray afterglow.

8.2.1. Black-hole formation without a quark-star stage

In the event that a black-hole is formed immediately following the core collapse, a collapsar scenario can occur if there is sufficient angular momentum present. Simulations of this scenario by De Villiers et al. (2005) show that an ultrarelativistic jet is launched

⁴This scenario is initially similar to that leading to a GRB with an associated hypernova, only that in this case the ejected material does not have enough energy to escape the star.

that can give rise to internal shocks and a GRB. In addition to the jet, a coronal wind was launched that could explode the remainder of the star. However, the energy of this wind was of the order $10^{48} - 10^{49}$ erg, which is not enough to explain a supernova. Hence this could be another possibility for explaining supernova-less GRBs, as discussed above. The duration of the accretion process is short (accretion rate of the order $1M_{\odot} \text{ s}^{-1}$ leading to a rather short duration GRB).

An alternative occurs when the coronal wind is not strong enough to explode the star. The star will then collapse, and assuming that it has high angular momentum, it will form a massive accretion disk around the black-hole. The accretion rate onto the black-hole is probably of the same order as with a smaller disk, however with much more mass to accrete this could lead to a somewhat longer duration jet and GRB. This resembles the original failed supernova discussed by Woosley (1993).

Both cases discussed above lead to a one stage model resulting in the absence of late time activity. Therefore, there will be no flares or bumps in the afterglow light curve, but flattening is still possible.

8.3. Collapsar vs. accreting quark-star as inner engine for GRBs

In this section we will briefly discuss the differences and similarities between our model and the collapsar model (Woosley 1993) for the inner engine for GRBs.

Similarities: Both the collapsar and our model assume the death of a massive, rapidly rotating star as the triggering mechanism. Both models launch an ultrarelativistic jet, in which internal shocks accelerate electrons that produce synchrotron radiation. As this jet is decelerated by the ISM, an external shock forms in which electrons again are accelerated and emit synchrotron emission that is responsible for the afterglow.

Differences: The collapsar model assumes that the compact core left behind in the collapse of the core of the progenitor star quickly collapses to a black-hole, whereas in our model this compact core collapses to a quark star instead. This opens up some interesting possibilities. The accretion rate into a black-hole and a quark-star are totally different. Accretion into a black-hole is a very rapid process, with accretion rates of the order of one solar mass per second. Accretion onto a quark star on the other hand is much slower (about 10^4 times slower). This can therefore easier explain the long duration (~ 1000 seconds) seen in some bursts. A main focus of this paper is the flaring often seen in the X-ray afterglow, which is indicative of the engine being restarted. With a quark-star the possibility of it collapsing to a black-hole exists, which explains how the inner engine can be restarted leading

to the observed features in the early X-ray afterglow.

9. Summary and conclusion

To summarize, the properties of the three stages of the inner engine in our model are:

- The process is initiated by the collapse of the iron core of a massive, rapidly rotating star.
- The collapsed core will either leave a neutron star or a quark-star behind.
- If a neutron star is left behind, it can collapse to a quark-star at a later stage, creating a delay between the supernova and the GRB.
- Fallback material from the supernova and the quark nova forms a disk around the quark-star. Accretion onto the quark-star generates the GRB by powering an ultrarelativistic jet. Internal shocks in this jet create the GRB.
- Accretion continues, but at some point it cannot heat up the star sufficiently. This halts the emission of shells, ending the GRB.
- When the quark-star has accreted too much material, it collapses into a black-hole. Further accretion onto the black-hole launches an ultrarelativistic jet.

The emission features in our model can be summarized as follows:

- Early, steep decay in the X-ray afterglow is due to the curvature effect (this is not specific to our model, but rather a generic feature in many models).
- Flares are created by interaction between the jet from the accretion onto a black-hole and slower parts from the jet from the quark-star.
- Re-energization of the external shock (seen as flattening of the X-ray afterglow light curve) is due only to the jet from the quark-star. Slower parts of this jet re-energizes the external shock.
- When the jet from the black-hole collides with the external shock from the GRB, a bump is seen in the afterglow light curve.

In conclusion, we have presented a three stage (effectively two stage) model for the inner engine for GRBs involving a neutron star phase, followed by a quark star phase then by a black hole phase. This model seems to account for the observed prompt gamma ray emission, as well as the features of the early X-ray afterglow and as such warrants further study.

We would like to thank J. Hjorth, M. Lyutikov M. Cummings, W. Dobler, D. Leahy and B. Niebergal as well as the anonymous referee for helpful remarks.

A. Internal-external shocks model

Piran (2005) shows that the pulse width is proportional to the separation between two shells:

$$\delta t \approx R_s/2a\Gamma^2c = L/ac \quad \text{equal mass shells,} \quad (\text{A1})$$

where R_s is the distance at which the collision takes place, a is the ratio between the fast and slow shells Lorentz factor, Γ the Lorentz factor of the slow shell, L the separation of the shells and c the speed of light. Assuming that the colliding shells have equal mass, and the faster has a Lorentz factor two times the slower shell, the separation between the two shells must be 3×10^{13} cm in order to have a pulse width of 500 seconds. This corresponds to a thousand seconds separation between the emission of the two shells.

The shells will collide at a distance

$$R_s \approx 2\Gamma^2L \quad (\text{A2})$$

where Γ refers to the Lorentz factor of the slower shell. For $\Gamma = 20$ and a separation of 3×10^{13} cm as before, the collisions occur at $R_s = 2 \times 10^{16}$ cm. If the Lorentz factors are too big, the external shocks will occur before internal shocks could occur. If the photon energy is large enough to produce e^+e^- pairs, the Lorentz factors of the shells have to be above a hundred to overcome the compactness problem. However, if the shocks creates X-rays, the photons cannot create e^+e^- pairs, and there is no lower bound on the Lorentz factor.

The internal energy of the merged shell is given by:

$$E_{\text{int}} = m_r c^2 (\Gamma_r - \Gamma_m) + m_s c^2 (\Gamma_s - \Gamma_m), \quad (\text{A3})$$

where m_r is the mass of the rapid shell, m_s of the slow shell, Γ_r is the Lorentz factor of the rapid shell, Γ_s is the Lorentz factor of the slower shell and Γ_m of the merged shell:

$$\Gamma_m = \sqrt{\frac{m_r \Gamma_r + m_s \Gamma_s}{m_r/\Gamma_r + m_s/\Gamma_s}}. \quad (\text{A4})$$

A certain fraction of this energy will be emitted as radiation. In order to have an efficient collision (a collision in which a lot of energy is converted to internal energy), the masses must be similar, and the Lorentz factor of the fast shell must be at least twice that of the slower shell. For a mass of the rapid shell of about 3×10^{28} g, which is not unlikely in a black-hole jet ($\dot{M} \sim 10^{-5} M_{\text{disk}}/s$ in De Villiers et al. 2005), and a mass of the slow shell of 3×10^{27} g, Lorentz factor of the rapid shell of $\Gamma_r = 65$, and Lorentz factor of the slow shell of $\Gamma_s = 20$, which gives $\Gamma_m = 57$ and an internal energy of about 10^{50} erg in a collision.

REFERENCES

- Alcock, C., Farhi, E., & Olinto, A. 1986, ApJ, 310, 261
- Bagchi, M., Ouyed, R., & Staff, J. E., Ray, S., Dey M., Dey J., 2006, astro-ph/0607509.
- Beloborodov, A. M., Stern, B. E., & Svensson, R., 2000, ApJ, 535, 158.
- Burrows, D. N., et al., 2005, Science, 309, 1833
- Dai, Z. G., Wang, X. Y., Wu, X. F., Zhang, B., 2006, Science, 311, 1127
- De Villiers, J. P., Staff, J. E., & Ouyed, R., 2005, astro-ph/0502225.
- Della Valle, M. “16th Annual October Astrophysics Conference in Maryland”, eds. S. Holt, N. Gehrels and J. Nousek, AIP Conf. Procs. astro-ph/0604110
- De Pasquale, M., et al., 2006, MNRAS, 365, 1031
- Falcone, A. D., et al., 2006, ApJ, 641, 1010.
- Frank, J., King, R., Raine, & D. J. 1992, Accretion Power in Astrophysics (Cambridge: Cambridge Univ. Press)
- Fryer, Ch. L., Benz, W., Herant, M. 1996, ApJ, 460, 801
- Fynbo, J., et al. 2006, Nature, 444, 1047
- Galama, T. J., et al. 1998, Nature, 395, 670
- Gehrels, N., et al. 2004, ApJ, 611, 1005
- Godet, O., et al., 2006, A&A, 452, 819
- Harko, T., Cheng, K. S., 2002, A&A, 385, 947

- Hjorth, J. et al., 2003, *Nature*, 423, 847
- Itoh, N, 1970, *PThPh*, 44, 291
- Iwazaki, A. 2005, *PhRvD*, 72, 114003
- Keränen, P., Ouyed, R., & Jaikumar, P., 2005, *ApJ*, 618, 485
- Kluźniak, W., Ruderman, M., 1998, *ApJL*, 505, 113
- Kobayashi, S., Piran, T., & Sari, R., 1997, *ApJ*, 490, 92
- Kumar, P. & Panaitescu, A. 2000, *ApJ*, 541,L51
- Liang, E. W., et al., 2006, *ApJ*, 646, 351
- Mazzali, P., et al., 2002, *ApJ*, 572, L61
- Mészáros, P. , 2006, “16th Annual October Astrophysics Conference in Maryland”, eds. S. Holt, N. Gehrels and J. Nousek, *AIP Conf. Procs.* astro-ph/0601661
- Narayan, R., Paczynski, B., & Piran, T., 1992, *ApJ*, 392, L83
- O’Brien, et al., 2006a, *ApJ*, 647, 1213
- O’Brien, P. T., Willingale, R., Osborne, J. P., & Goad, M. R., 2006b, *NJPh*, 8, 121.
- Ouyed, R., Dey, J., & Dey, M. 2002, *A&A*, 390, 39
- Ouyed, R., Rapp, R., & Vogt, C., 2005, *ApJ*, 632, 1001 (ORV).
- Ouyed, R., Niebergal, B., Dobler, W., & Leahy, D., 2006, *ApJ*, 653, 558.
- Panaitescu, A., Mészáros, P., Burrows, D., Nousek, J., Gehrels, N., O’Brien, P., & Willingale, R. 2006, *MNRAS*, 369, 2059
- Piran, T., 1999, *PhR*, 314, 575
- Piran, T., 2005, *Rev. Mod. Phys.*, 76, 1143.
- Popham, R., Woosley, S.E., & Fryer, Ch. 1999, *ApJ*, 518, 356.
- Rhoads, J. E. 1999, *ApJ*, 525, 737.
- Ruderman, M. A., Tao, L., Kluźniak, W., 2000, *ApJ*, 542, 243
- Sari, R. & Mészáros, P. 2000, *ApJ*, 535, L33.

- Staff, J., Ouyed, R., & Jaikumar, P. 2006, *ApJ*, 645, L145
- Tagliaferri, G. et al., 2005, *Nature*, 436, 985
- Tominaga, N., Maeda, K., Umeda, H., Nomoto, K., Tanaka, M., Iwamoto, N., Suzuki, T. & Mazzali, P. A., 2007, *ApJ*, 657, L77.
- Usov, V. V. 1992, *Nature*, 357, 472
- Vogt, C., Rapp, R., & Ouyed, R. 2004, *Nuc. Phys. A*, 735, 543.
- Wheeler, J. C., Yi, I., Höflich, P., Wang, L., 2000, *ApJ*, 537, 810.
- Woosley, S.E. 1993, *ApJ*, 405, 273.
- Zhang, B., Fan, Y.Z., Dyks, J. Kobayashi, S., Mészáros, P., Burrows, D.N., Nousek, J.A., & Gehrels, N. 2006, *ApJ*, 642, 354.
- Zhang, B, Zhang, B. B., Liang, E. W., Gehrels, N., Burrows, D. N. & Mészáros, P. 2007, *ApJ*, 655, L25.
- Zou, Y. C., Dai, Z. G., & Xu, D. 2006, *ApJ*, 646, 1098.

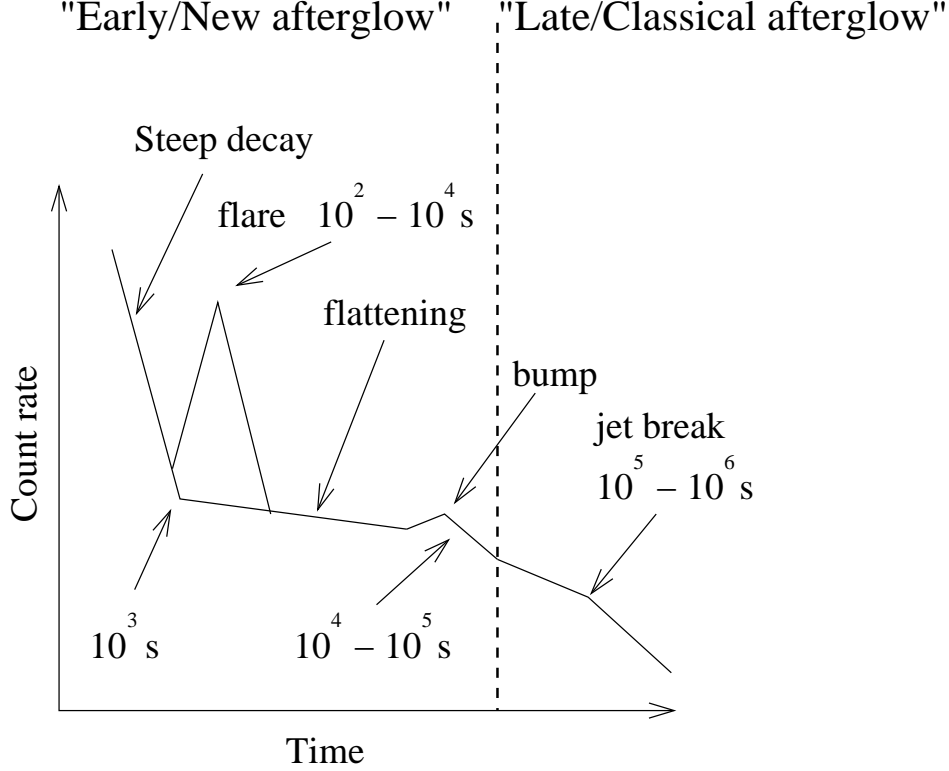


Fig. 1.— Generic X-ray afterglow (e.g. Zhang et al. 2006). At early times ($t < 1000$ seconds), a steep decay is often seen, followed by a flattening starting at $t = 10^3$ and lasting for about $10^4 - 10^5$ seconds. Thereafter a steeper decay, and after about a day or so a new break is seen. The last break is termed “jet break”. On top of this one or more flares are often observed between $t = 10^2 - 10^4$ seconds, and one or more bumps can be seen between $t = 10^4$ seconds and $t = 10^5$ seconds. **NOTE:** Not all features are seen in every bursts. Before (the launch of the) Swift satellite, the part of the figure including the steep decay, the flares and the flattening was essentially unobserved.

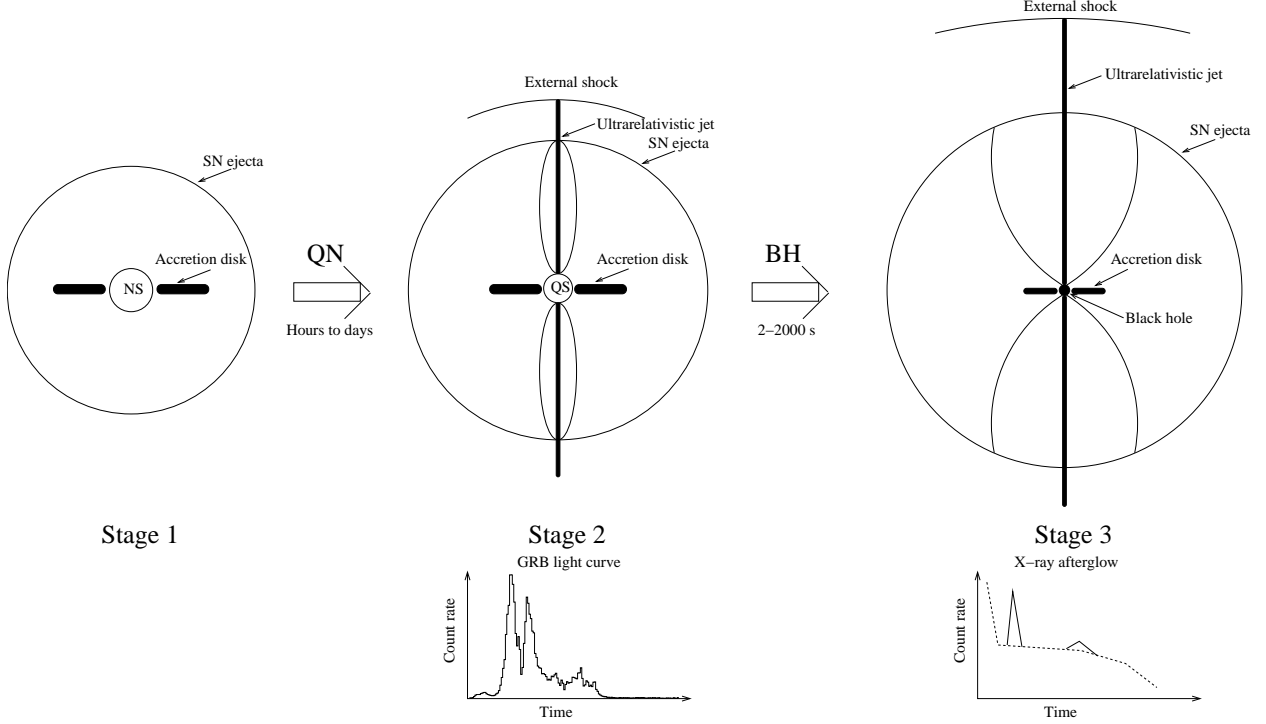
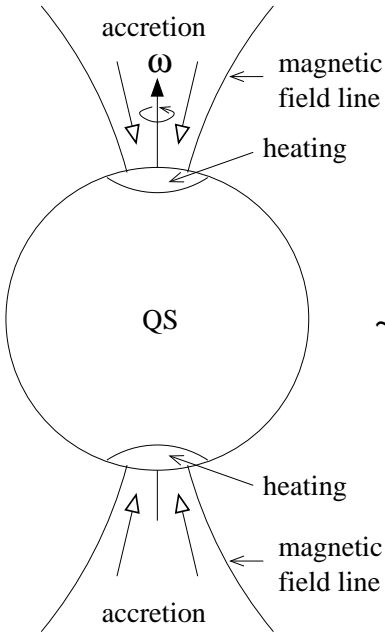


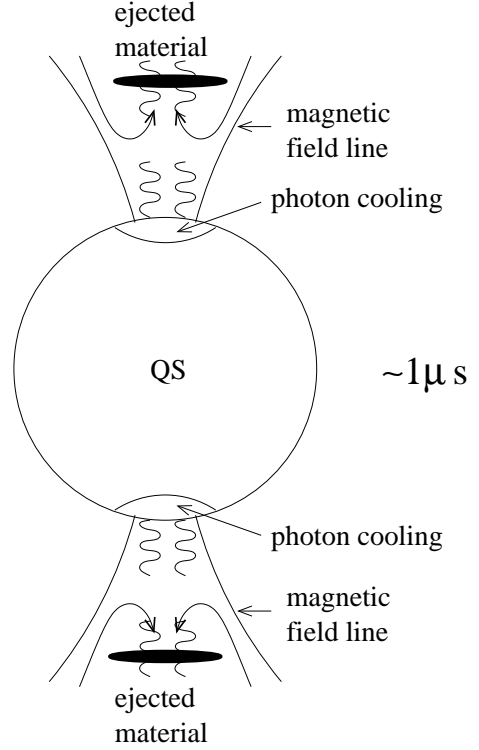
Fig. 2.— The three stages in a GRB inner engine. *Stage 1:* A neutron star is formed in the core collapse of a massive star. The neutron star can later collapse into a quark-star due to spin-down or accretion. If this takes a long time, it will cause a delay between the supernova and the GRB. *Stage 2:* A quark-star in the CFL phase is formed, either directly in the supernova, or from the neutron star in Stage 1. Accretion onto this star heats the star, leading to emission of photons as the main cooling mechanism. If the star is heated above the plasma frequency of about 7.7 MeV (ORV), the photons can escape the star and will interact with the accreting matter. The infalling matter is ejected, leading to a halt in the accretion process. When the star cools down below 7.7 MeV, accretion can be resumed. This creates episodes of accretion and ejection. Internal shocks created from colliding shells in the ejected material create the GRB. *Stage 3:* At later stages in the accretion process the accretion may not be strong enough to heat the star above 7.7 MeV. This prevents ejection of material, and hence terminates the GRB. However, the accretion will continue. If the star accretes too much matter, it will collapse to a black-hole. This dramatically changes the accretion, and launches an ultrarelativistic jet. This jet will interact with slower parts of the jet from the quark-star, leading to internal shocks. This creates the flares often seen in the early X-ray afterglow. When the jet from the black-hole collides with the external shock, a bump is observed on the light curve.

Accretion/Heating



$\sim 1\text{ms}$

Ejection/Cooling



$\sim 1\mu\text{s}$

Fig. 3.— Cartoon illustrating the jet launching mechanism in our model. Infalling material follows magnetic field lines to the polar cap (magnetic pole is at the same location as the geographic pole in a CFL star, see text), where it heats the star. The timescale for heating the star is of the order milliseconds. The star then cools by emitting photons on a timescale of the order of microseconds. These photons interact with the infalling material, ejecting some of that with large Lorentz factors.

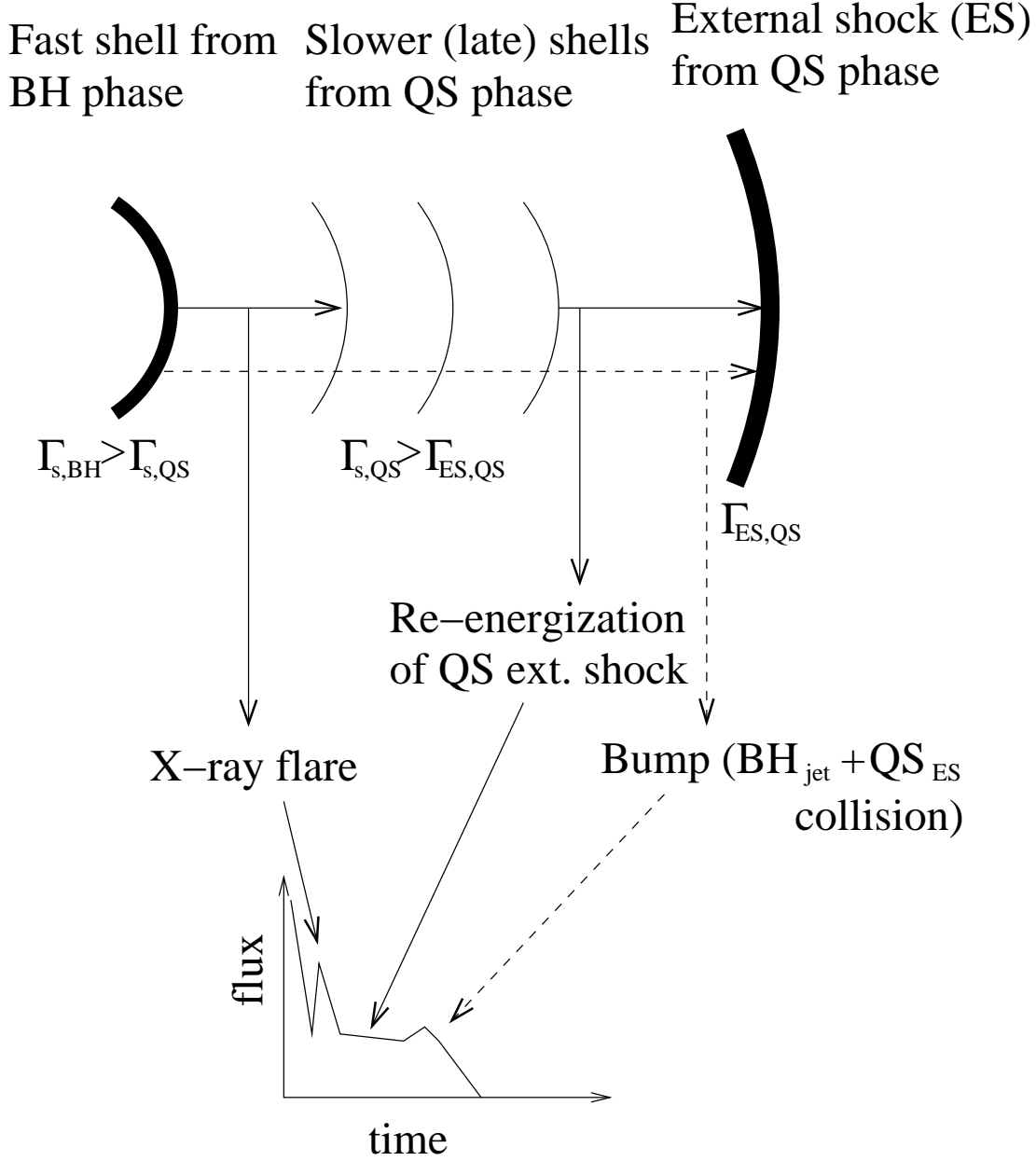


Fig. 4.— Illustration of the mechanism leading to X-ray flares and flattening of the X-ray afterglow light curve. In both cases, the quark-star needs to emit low-Lorentz factor shells in the late stages of shell emission. When these shells collide with the external shock from the GRB, that shock is re-energized and a flattening of the light curve results. If the quark star accretes too much mass, it will collapse to a black-hole. The jet emitted in the accretion process onto the black-hole can be massive and have a high Lorentz factor. When this outflow collides with a slow shell from the quark-star, an X-ray flare results. If this merged shell collides with more low-Lorentz factor shells from the quark-star, more flares will result. A bump can be seen when the black-hole ejecta collide with the external shock.

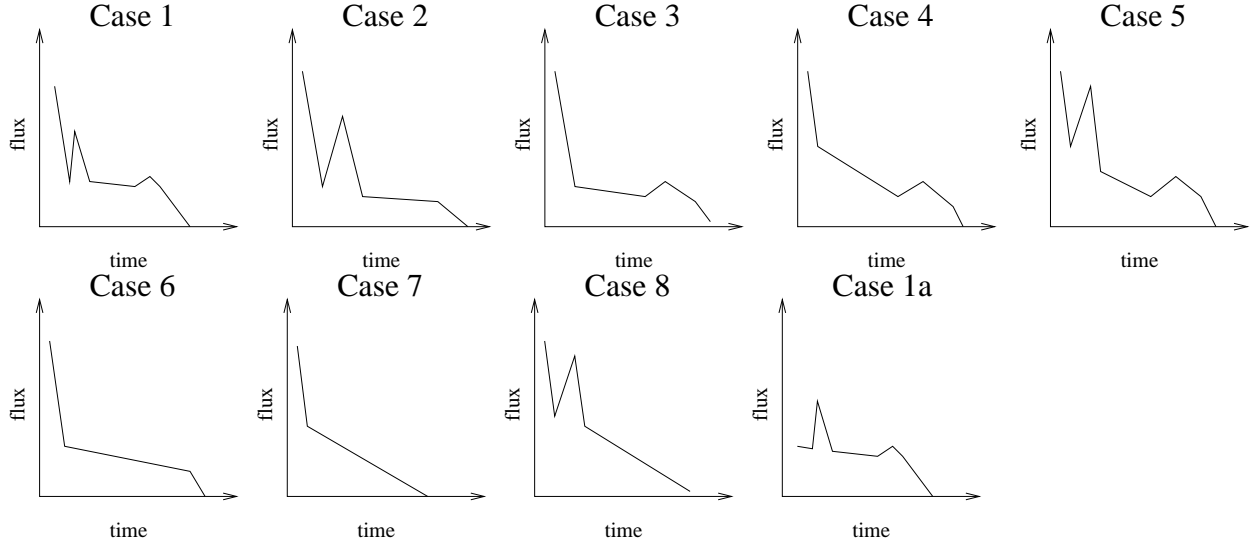


Fig. 5.— The different kinds of light curves derived from our model. Case 1 is also illustrated in Fig. 4. There are flares, flattening and a bump. This occurs when the quark-star jet produces slow shells that can re-energize the external shock. The black hole jet interacts with some of these shells and creates flares. When the merged black-hole jet collides with the external shock, the bump is formed. *Case 2*: We see one or more flares and a flattening of the light curve, but no bump. This is because the shell from the black-hole is slowed down so much by the other shells from the quark-star that it reaches the external shock at very late times. *Case 3*: Flattening and a bump, but no flare. The shell from the black-hole did not collide with any shell and therefore did not create a flare. It creates a bump when it collides with the external shock. *Case 4*: No flare, no flattening, but a bump. The quark-star jet did not contain any late time shells, so there were no flattening and no flare created. As in Case 3, the black-hole jet creates a bump when it collides with the external shock. *Case 5*: Flare and bump, but no flattening. There are only a few late time shells emitted from the quark-star. The black hole jet collides with these and creates flares. When this merged shell collides with the external shock a bump is seen. No late time shells can flatten the light curve. *Case 6*: No flares, no bump but flattening. The quark-star emits late time shells that flattens the light curve. No black-hole was formed. *Case 7*: No flares, no bump, no flattening. No black-hole was formed, and the quark-star did not emit any late time shells. *Case 8*: Flares, but no bump and no flattening. This indicates that a black-hole which launched an ultrarelativistic jet was formed, but in the process of forming the flares this jet was slowed down enough so that it cannot energize the external shock to generate a bump. *Case 1a*: Same as case 1, but no early steep decay. All cases from 1 to 8 can exist without the early steep decay as illustrated in case 1a where the decay is absent for case 1. Note that a possible break in the light curve due to collimation of the outflow producing the GRB and the afterglow will occur at later times than what is shown in this figure.

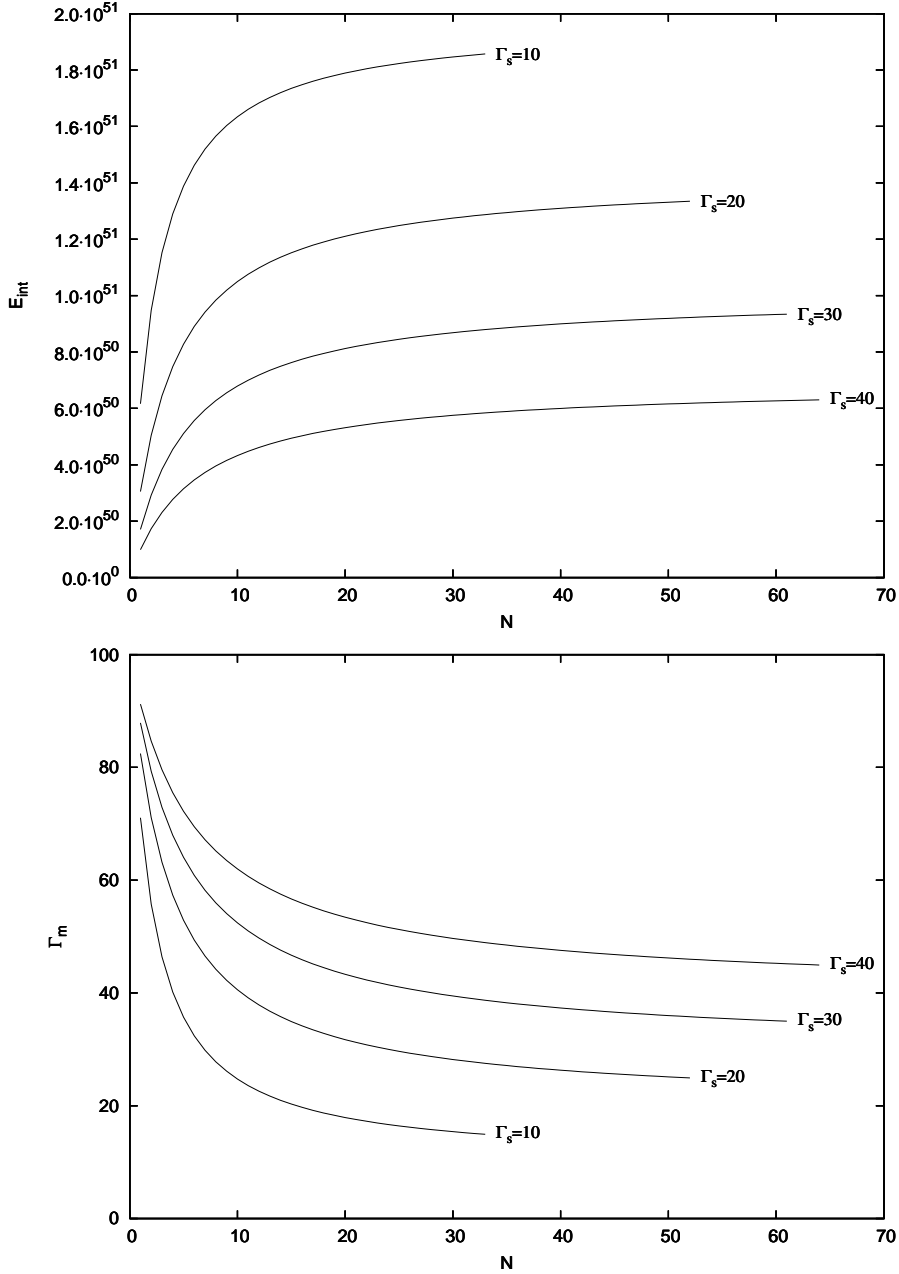


Fig. 6.— Figure showing the total energy converted to internal energy versus number of collisions (upper panel) and the Lorentz factor of the merged shell versus number of collisions (lower panel). In all cases the rapid shell has a Lorentz factor of 100 initially, and all the slow shells have Lorentz factors of 10, 20, 30 or 40 respectively. The mass of the rapid shell is 3×10^{28} g, and the mass of the slow shells are 3×10^{27} g. The figures show that after 10 to 20 collisions a plateau is reached and no more energy is converted. The Lorentz factor reaches a plateau. In this plateau, collisions can still occur, so the merged shell can gain mass. When the slower shells have higher Lorentz factors, the merged shell ends up with a higher Lorentz factor after the collisions, and the energy conversion is reduced. This leaves more energy to be converted when this merged shell collides with the preceding quark-star external shock.